AIP | Applied Physics Letters

Photocarrier localization and recombination dynamics in Cu2ZnSnS4 single crystals

Le Quang Phuong, Makoto Okano, Yasuhiro Yamada, Akira Nagaoka, Kenji Yoshino, and Yoshihiko Kanemitsu

Citation: Applied Physics Letters **103**, 191902 (2013); doi: 10.1063/1.4829063
View online: http://dx.doi.org/10.1063/1.4829063
View Table of Contents: http://scitation.aip.org/content/aip/journal/apl/103/19?ver=pdfcov
Published by the AIP Publishing

Photocarrier localization and recombination dynamics in Cu_2ZnSnS_4 single crystals

Le Quang Phuong,[1,2] Makoto Okano,[1] Yasuhiro Yamada,[1] Akira Nagaoka,[3] Kenji Yoshino,[3] and Yoshihiko Kanemitsu[1,2,a)]
[1]*Institute for Chemical Research, Kyoto University, Uji, Kyoto 611-0011, Japan*
[2]*Japan Science and Technology Agency, CREST, Uji, Kyoto 611-0011, Japan*
[3]*Department of Applied Physics and Electronic Engineering, University of Miyazaki, Miyazaki 889-2192, Japan*

(Received 7 October 2013; accepted 22 October 2013; published online 5 November 2013)

We have studied the photocarrier localization and recombination dynamics in Cu_2ZnSnS_4 single crystals at room temperature. The band-gap energy and tail states below the band edge were evaluated by a combination of photoluminescence (PL), PL excitation, photocurrent, and femtosecond transient reflectivity spectroscopy. The photocarriers are rapidly localized to shallow tail states within a typical time constant of several picoseconds to a few tens of picoseconds. The sub-nanosecond PL decay dynamics indicate the importance of multiple carrier trapping processes in the shallow tail states. Therefore, it is concluded that the tail states dominate the optical responses of Cu_2ZnSnS_4 single crystals. © *2013 AIP Publishing LLC*.
[http://dx.doi.org/10.1063/1.4829063]

Recently, there have been extensive studies on the fabrication and optoelectronic properties of quaternary semiconductor compounds, such as $CuIn_{1-x}Ga_xSe$ (CIGS), because their band-gap energies are optimal for solar energy conversion and they have high optical absorption coefficients in the near-infrared and visible spectral regions. In particular, Cu_2ZnSnS_4 (CZTS), which is composed of only earth-abundant elements, is attracting considerable attentions as a less-toxic and low-cost absorber material for solar cells.[1–5] The best solar energy conversion efficiency of CZTS-based solar cells obtained to date is about 8.4%,[6] which is still much lower than the high conversion efficiency of 20.3% obtained for CIGS thin-film solar cells.[7] To improve the conversion efficiency of CZTS-based solar cells, it is important to obtain more detailed information of the fundamental physical properties on CZTS material itself.

Many efforts have been made to investigate the fundamental optical and electronic properties of CZTS.[3,8–19] Photoluminescence (PL) spectroscopy is widely used to reveal the mechanisms of photocarrier recombination in CZTS samples.[11–19] An asymmetric, broad PL band located around 1.3 eV at low temperatures has been reported in recent work,[11–15] the origin of which has been discussed in terms of donor-acceptor pair (DAP) recombination or a free-to-bound (FB) transition with a large thermal activation energy.[11,12,15] The band-edge potential fluctuation model has also been proposed to explain the large peak shifts in response to the excitation density and temperature.[13,14,19] The origin of the PL band, therefore, is still under discussion. Note that most previous experimental reports dealt with polycrystalline CZTS thin films with grains, which might obscure some intrinsic PL features. In addition, there are very few reports discussing the PL mechanism in CZTS at room temperature (RT) because of the weak PL from CZTS samples.

One important step in determining the photocarrier recombination mechanisms in any optical material is to identify its band-gap energy and to understand its optical response around the band-gap energy. So far, only the band-gap energy of polycrystalline CZTS thin films has been reported experimentally by means of optical absorption spectroscopy.[1,17,18] However, for CZTS single crystals, optical absorption measurement is not a simple task because the high absorption coefficient leads to great challenges in the preparation of high-quality, thin, crystalline samples. In addition, an unintentionally high concentration of impurities and defects in quaternary CZTS samples forms a large density of tail states below the band edge. These cause difficulties for experimental efforts to obtain reliable values of the band-gap energy.

In this Letter, we clarify the photocarrier localization and recombination dynamics in CZTS single crystals at RT. The band-gap energies was identified consistently by various means, including PL excitation (PLE), photocurrent (PC), and transient reflectivity spectroscopy and was estimated to be approximately1.58 eV at RT. The PL band was assigned to radiative recombination of carriers localized in shallow trap states. It was found that free photocarriers in CZTS are localized to trap states within a few tens of picoseconds. The time-resolved PL measurements revealed power-law-dependent recombination dynamics, indicating the occurrence of multiple carrier trapping processes near the band edge.

The CZTS single crystals investigated in this study were grown using the traveling heating method.[20] The composition of the CZTS single crystals was estimated from the stoichiometric ratio to be slightly Cu-poor, Zn-rich, Sn-poor, and S-rich. The Cu-poor, Zn-rich, and S-rich composition is believed to be important for obtaining highly efficient CZTS solar cells.[4,6,22]

a)Author to whom correspondence should be addressed. Electronic mail: kanemitu@scl.kyoto-u.ac.jp

In steady and time-resolved PL measurements, the excitation pulse emitted from an optical parametric amplifier pumped by a Yb:KGW (potassium gadolinium tungstate) regenerative amplified laser with a pulse duration of ~300 fs and a repetition rate of 200 kHz was focused onto the samples' surfaces with a spot size of ~100 μm. The excitation photon energy was tuned to 2.06 eV, which is well above the band-gap energy of CZTS. The PL signal was collected in a backward configuration and directed to the entrance slit of a 50-cm monochromator equipped with a liquid-nitrogen-cooled Si CCD. The spectral responses of all PL measurements were calibrated using a standard lamp.

The time-resolved PL measurements were performed using a near-infrared streak camera. The temporal resolution of our system was about 20 ps. In white-light pump-probe transient reflectivity measurements, the same excitation source utilized in PL measurements was chopped by an optical chopper with a frequency of 130 Hz and then used as a pump pulse. Part of the seed pulse from the Yb:KGW regenerative amplified laser was focused on a sapphire crystal to generate a white-light probe pulse. The reflection of the probe pulse was collected through a monochromator.

In PC and PLE measurements, a wavelength-tunable continuous-wave Ti:sapphire laser was used as the excitation source, and the excitation photon energy was tuned from 1.37 to 1.72 eV. The PL signal was detected by a liquid nitrogen-cooled InGaAs photodiode array through a 30-cm monochromator, although the photocurrent was converted to voltage and then collected by a lock-in amplifier. All measurements were performed at RT.

Figure 1 shows the PL, PC, and PLE spectra of the CZTS single crystal sample obtained at RT. The PL spectrum was measured under a pulse laser excitation of 7.5 μJ/cm^2. The PC and PLE measurements were performed simultaneously under weak excitation conditions, and the PL spectral shape was confirmed to be independent of the excitation photon energy. As shown in Fig. 1, the PC and PLE spectra have similar shapes. Both the PC and PLE spectra show large tails in the low-excitation-energy region, then gradually rise to reach peaks at ~1.62 eV, and finally decrease in the higher-excitation-energy regions. A similar response was observed for the photocurrent at excitation energies larger than the absorption edge in not-so-high-quality II-VI and III-V semiconductor compounds such as CdS, InSb, InAs, and GaSb.[23–25] Based on these previous reports, the decrease in the PC and PLE spectra of CZTS single crystals at the high excitation energies might be assigned to increasing surface recombination.[26,27] Because of the short optical penetration depth of high-energy photons, they produce carriers in the near-surface layers of the CZTS sample. Large nonradiative surface recombination rates become dominant under high-photon-energy excitation, leading to a decrease in the PLE and PC signals.[26,27] The peaks in the PC and PLE spectra at ~1.62 eV indicate that strong optical absorption corresponding to the band-to-band transition occurs at around 1.62 eV, so the band edge of CZTS at RT must be located near ~1.62 eV. However, the observed large tails of the PC and PLE spectra at low excitation energies might make it difficult to determine exactly where the band-gap energy of CZTS single crystals is.[18] To determine the band-gap energy more precisely, we show below another identification of the band-gap energy from transient reflectivity spectra.

A broad PL band appears in the low-energy side of the PC and PLE spectra, with a peak at ~1.35 eV, as shown in Fig. 1. As mentioned previously, a large density of tail states due to impurities and defects causes noticeable PC and PLE signals on the low-energy side of the band-gap energy. The broad PL band and the large Stokes shift indicate that tail states below the band edge might be involved into the PL processes in CZTS single crystals. The excitation density dependence of the time-integrated PL spectrum is displayed in Fig. 2(a). With increasing the excitation density, the peak energy shows a large blueshift of several tens of meV per excitation density decade. The PL intensity is presented as a function of the excitation density in Fig. 2(b). The PL intensity depends linearly on the excitation density in the weak excitation region and then tends to be saturated in the strong excitation region. This saturation tendency of the PL intensity is due to the filling up of the shallow tail states involved in the PL process.

To explain the large peak shift (larger than 10 meV per excitation intensity decade), the potential fluctuation model has been adopted.[13,14,19] In highly doped materials, shallow energy structures no longer form discrete levels but instead form a continuum band. In fact, Hall measurements made

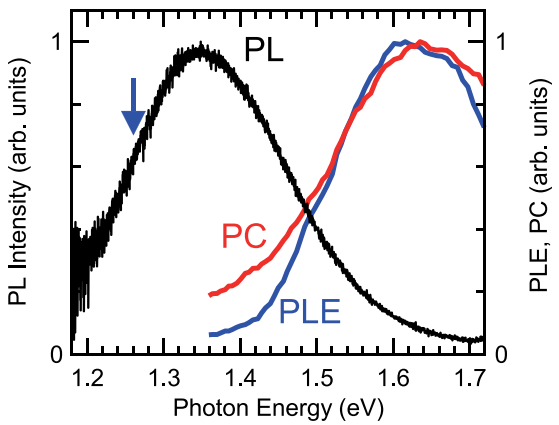

FIG. 1. PL (black line), PC (red line), and PLE (blue line) spectra of CZTS single crystals at room temperature. The arrow indicates the energy monitored for PL excitation spectrum.

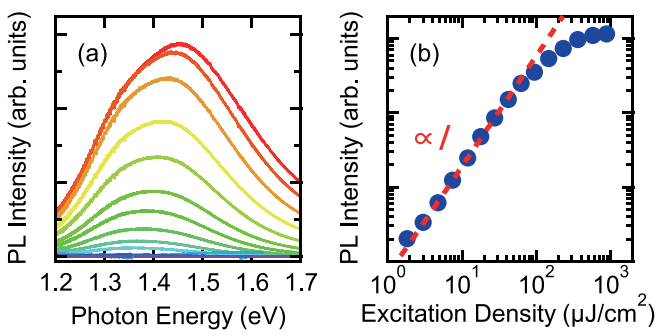

FIG. 2. (a) Time-integrated PL spectra of CZTS single crystals at various excitation densities (from 1.8 μJ/cm^2 to 880 μJ/cm^2) measured at room temperature. (b) PL intensity as a function of the excitation density (solid circles). The dashed line shows the linear fitting result in the weak excitation region.

using the van der Pauw method at RT have revealed rather high hole carrier concentrations of $\sim 10^{16}$–10^{17} cm^{-3} in the studied CZTS single crystals.[20,21] Therefore, it is plausible to propose that donor and acceptor bands form in our CZTS single crystals,[21] and thus the observed PL band is proposed to be due to radiative recombination of carriers localized in the donor and acceptor bands. Under strong excitation conditions, the carriers occupy high-energy tail states, and the emission energy of the radiative recombination of carriers localized in the donor and acceptor bands shifts drastically to the high-energy side.

To gain a deeper understanding of the photocarrier dynamics in the band tail states, we have made the transient reflectivity and time-resolved PL measurements of our samples. Figure 3 shows a contour image of a typical white-light pump-probe transient reflectivity spectrum. Because of the fast state filling by carriers excited by the pump pulse,[28,29] bleaching (positive) signals are observed after photoexcitation for probe energies larger than ~1.6 eV. However, the transient reflectivity signals are more complicated for probe energies smaller than the band-gap energy and are typically composed of an induced absorption (negative) signal at early delay times and a bleaching signal at long delay times. The white solid circles in Fig. 3 show the peak of the bleaching signal as a function of the pump-probe delay time. The peak energy shows a large redshift just after photoexcitation, and then finally reaches an almost constant value of 1.58 eV after a delay time of about 200 ps, as shown by the dashed line in Fig. 3. The observed peak redshift of the bleaching signal reflects the energy relaxation of photocarriers into lower energy states. The inset in Fig. 3 shows the transient reflectivity spectrum at a delay time of 285 ps and its peak is located at 1.58 eV. Note that the photo-bleaching usually appears at the band-gap energy in direct band-gap semiconductors, and theoretical calculations predict that CZTS is a direct band-gap semiconductors.[8–10] Thus, it is reasonable to assign the peak energy of the bleaching signal, estimated to be about 1.58 eV as discussed above, to the band-gap energy of CZTS single crystals. This value is consistent with the approximation from the PLE and PC spectra shown in Fig. 1. Similar values of the band-gap energy have been predicted by theoretical calculations[8–10] and reported experimentally for CZTS polycrystalline thin films based on optical absorption spectroscopy.[1,17,18]

Next, we discuss the photocarrier dynamics in CZTS single crystals at RT. Figure 4 presents two typical time profiles of the transient reflectivity signals at probe energies of 1.42 eV (below the band-gap energy) and 1.71 eV (above the band-gap energy). The transient reflectivity bleaching signal for the probe energy larger than the band-gap energy could be fitted well by three exponential components with time constants of 2.5, 12, and 100 ps, as shown by the black solid line in Fig. 4. Although these three times constants depend on the probe photon energy, the two fast components are surely around picoseconds and a few tens of picoseconds, and the slow component is a few hundreds of picoseconds. Theoretical calculations were used to predict the simple band structures of CZTS,[10] which suggest that the intraband relaxations of excited carriers through phonon interactions might occur on order of femtoseconds as is the usual case in semiconductors.[30–32] In addition, because the studied CZTS single crystals are p-type and heavily doped semiconductors, the temporal change of the transient reflectivity signal is sensitive to the relaxation or localization of electrons. Hence, the two fast decay times of several picoseconds and a few tens of picoseconds are caused by the rapid relaxations of free electrons to the shallow trap states and rapid surface recombination. If we adopt the above-described relaxation picture for CZTS, the fast decay components of the bleaching signal for a probe energy larger than the band-gap energy should contribute rise-time components to the transient reflectivity signal detected at probe energies smaller than the band-gap energy. As shown in Fig. 4, a typical time profile of transient reflectivity signal at a probe energy smaller than

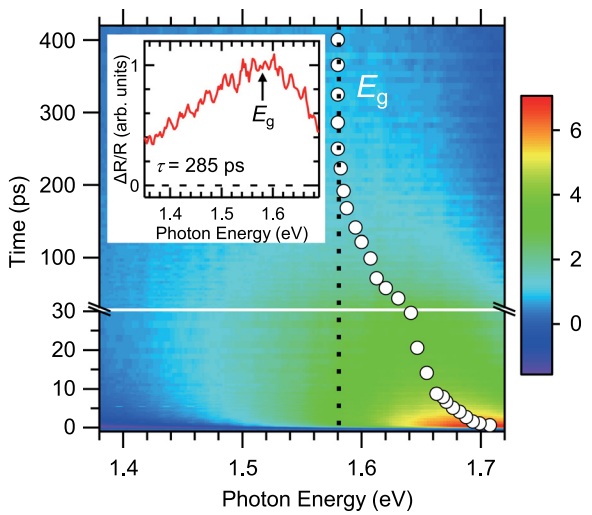

FIG. 3. Contour image of a typical white-light pump-probe transient reflectivity spectrum of the CZTS single crystal at room temperature. The white solid circles indicate the peak energies of the bleaching signals at different delay times. The dashed line displays the band-gap energy E_g of CZTS single crystals. The transient reflectivity spectrum at a delay time of 285 ps is shown in the inset.

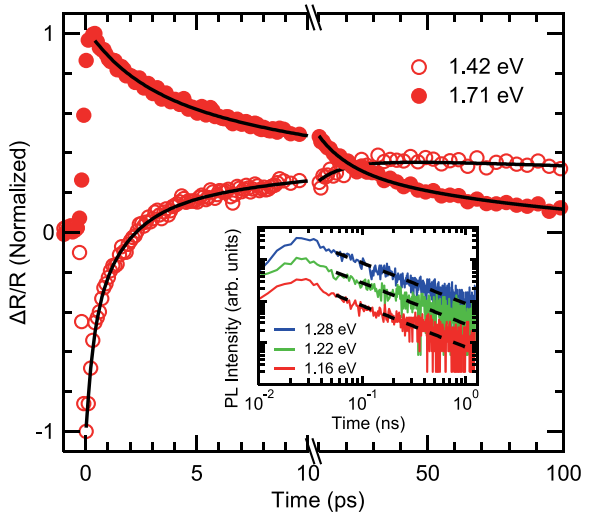

FIG. 4. Normalized time profiles of transient reflectivity spectra at two different probe energies of 1.42 eV (open circles) and 1.71 eV (solid circles) at room temperature. The solid lines show the fitting results using tri-exponential functions. The inset displays typical PL decay profiles at different emission energies. The dashed lines show the fitting results at the long-time part of the decay profiles, which follow power-law dependence t^{-m}.

the band-gap energy could, in fact, be reconstructed well by a combination of a positive two-rise-time bleaching component and a negative induced absorption component that is fixed to be proportional to the free-carrier induced absorption time profile at a probe energy of 0.85 eV, which is much smaller than the band-gap energy. Consequently, we obtain two rise-time components with typical values of several picoseconds and several tens of picoseconds, which are consistent with the obtained fast decay times of the transient reflectivity signals for probe energies larger than the band-gap energy. Therefore, we conclude that fast relaxation and localization of the photocarriers occur in CZTS single crystals.

Finally, we discuss the slowest decay time of a few hundreds of picoseconds observed in the transient reflectivity spectra. The inset in Fig. 4 shows log-log plots of typical PL decay profiles at three different emission energies. The decay times observed in the time-resolved PL measurements roughly agree with those found in the transient reflectivity measurements. The long-time part of the decay profiles can also be described approximately by a power-law dependence t^{-m}, as shown by the dashed lines in the inset ($m \sim 1$). The power-law-dependent recombination dynamics (t^{-m}) indicates that multiple trapping processes are essentially involved in the PL emission of CZTS single crystals.[33–35] The free photocarriers are captured rapidly and efficiently in trap sites composed of not only radiative but also a large number of nonradiative centers, which subsequently leads to the low PL efficiency of the CZTS samples at RT. The power-law-dependent dynamics of the PL process in CZTS single crystals means that a significant fraction of the carriers are still localized at trap sites for a long time, which reduces their contribution to the photocurrent or, in other words, limits the power conversion efficiency of the material.

In conclusion, we have clarified the photocarrier localization and recombination dynamics in CZTS single crystals. The large-density band tail states formed below the band edge of 1.58 eV determines the optical responses. The rapid photocarrier localization into shallow tail states will limit the conversion efficiency of CZTS-based solar cells. Our kinematic studies provide essential information relevant to the improvement of the power conversion efficiency of CZTS-based solar cells.

This work was supported by JST-CREST and the Sumitomo Electric Industries Group CSR Foundation.

[1]K. Ito and T. Nakazawa, Jpn. J. Appl. Phys., Part 1 **27**, 2094 (1988).
[2]H. Katagiri, K. Jimbo, W. S. Maw, K. Oishi, M. Yamazaki, H. Araki, and A. Takeuchi, Thin Solid Films **517**, 2455 (2009).
[3]S. Chen, X. G. Gong, A. Walsh, and S. H. Wei, Appl. Phys. Lett. **94**, 041903 (2009).
[4]K. Wang, O. Gunawa, T. Todorov, B. Shin, S. J. Chey, N. A. Bojarczuk, D. Mitzi, and S. Guha, Appl. Phys. Lett. **97**, 143508 (2010).
[5]C. Steinhagen, M. G. Panthani, V. Akhavan, B. Goodfellow, B. Koo, and B. A. Korgel, J. Am. Chem. Soc. **131**, 12554 (2009).
[6]B. Shin, O. Gunawan, Y. Zhu, N. A. Bojarczuk, S. J. Chey, and S. Guha, Prog. Photovoltaics **21**, 72 (2013).
[7]P. Jackson, D. Hariskos, E. Lotter, S. Paetel, R. Wuerz, R. Menner, W. Wischmann, and M. Powalla, Prog. Photovoltaics **19**, 894 (2011).
[8]A. Nagoya, R. Asahi, R. Wahl, and G. Kresse, Phys. Rev. B **81**, 113202 (2010).
[9]S. Chen, J. H. Yang, X. G. Gong, A. Walsh, and S. H. Wei, Phys. Rev. B **81**, 245204 (2010).
[10]C. Persson, J. Appl. Phys. **107**, 053710 (2010).
[11]K. Tanaka, Y. Miyamoto, H. Uchiki, K. Nakazawa, and H. Araki, Phys. Status Solidi A **203**, 2891 (2006).
[12]Y. Miyamoto, K. Tanaka, M. Oonuki, N. Moritake, and H. Uchiki, Jpn. J. Appl. Phys., Part 1 **47**, 596 (2008).
[13]J. P. Leitao, N. M. Santos, P. A. Fernandes, P. M. P. Salome, A. F. da Cunha, J. C. Gonzalez, G. M. Ribeiro, and F. M. Matinaga, Phys. Rev. B **84**, 024120 (2011).
[14]M. J. Romero, H. Du, G. Teeter, Y. Yan, and M. M. Al-Jassim, Phys. Rev. B **84**, 165324 (2011).
[15]S. Levcenko, V. E. Tezlevan, E. Arushnow, S. Schorr, and T. Unold, Phys. Rev. B **86**, 045206 (2012).
[16]M. Grossberg, J. Krustok, J. Raudoja, and T. Raadik, Appl. Phys. Lett. **101**, 102102 (2012).
[17]P. K. Sarswat and M. L. Free, Physica B **407**, 108 (2012).
[18]C. Malerba, F. Biccari, C. L. A. Recardo, M. Valentini, R. Chierchia, M. Muller, A. Santoni, E. Espotito, P. Mangiapane, P. Scardi, and A. Mittiga, J. Alloys Compd. **582**, 528 (2014).
[19]D. P. Halliday, R. Claridge, M. C. J. Goodman, B. G. Mendis, K. Durose, and J. D. Major, J. Appl. Phys. **113**, 223503 (2013).
[20]A. Nagaoka, K. Yoshino, H. Taniguchi, T. Taniyama, and H. Miyaka, J. Cryst. Growth **341**, 38 (2012).
[21]A. Nagaoka, H. Miyake, T. Taniyama, K. Kakimoto, and K. Yoshino, Appl. Phys. Lett. **103**, 112107 (2013).
[22]T. K. Todorov, K. B. Reuter, and D. B. Mitzi, Adv. Mater. **22**, E156 (2010).
[23]R. H. Bube, J. Chem. Phys. **21**, 1409 (1953).
[24]R. H. Bube, Phys. Rev. **101**, 1668 (1956).
[25]T. S. Moss, Rep. Prog. Phys. **28**, 15 (1965).
[26]J. Lambe, Phys. Rev. **98**, 985 (1955).
[27]R. H. Bube, Phys. Rev. **83**, 393 (1951).
[28]Z. Vardeny and J. Tauc, Phys. Rev. Lett. **46**, 1223 (1981).
[29]T. Elsaesser, J. Shah, L. Rota, and P. Lugli, Phys. Rev. Lett. **66**, 1757 (1991).
[30]W. Z. Lin, L. G. Fujimoto, E. P. Ippen, and R. A. Logan, Appl. Phys. Lett. **50**, 124 (1987).
[31]T. Sjodin, H. Petek, and H. Dai, Phys. Rev. Lett. **81**, 5664 (1998).
[32]A. J. Sabbah and D. M. Riffe, Phys. Rev. B **66**, 165217 (2002).
[33]Y. Yamada and Y. Kanemitsu, Appl. Phys. Lett. **101**, 133907 (2012).
[34]H. Scher and E. W. Montroll, Phys. Rev. B **12**, 2455 (1975).
[35]T. Tiedje and A. Rose, Solid State Commun. **37**, 49 (1981).